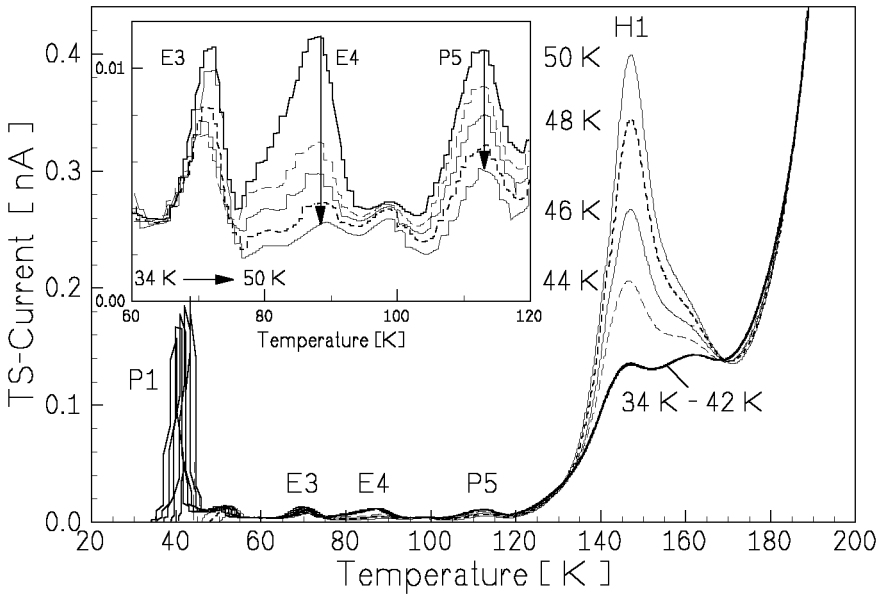

Figure 7.28: TSC-spectra with filling temperature as parameter (sample : MUEA06). Peak P1 can not be analysed, because it consists of only few points.

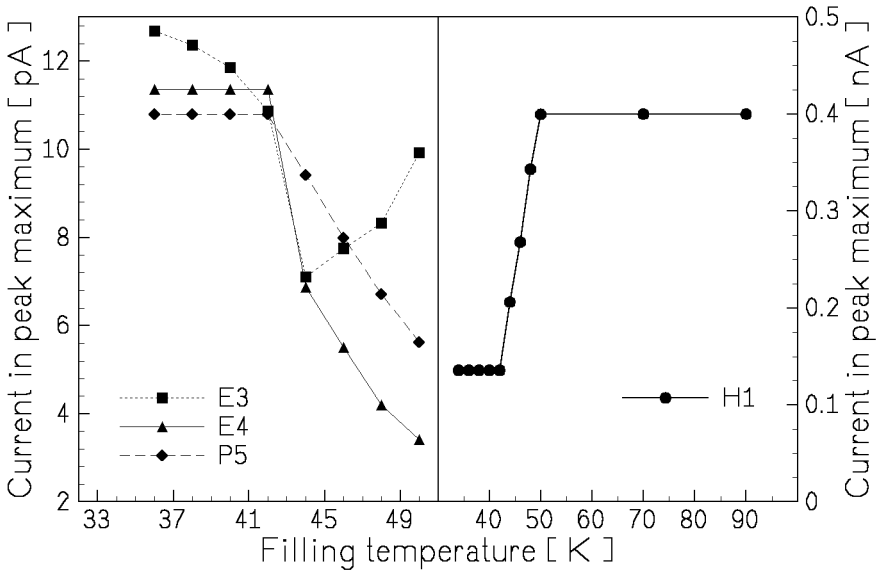

Figure 7.29: Maxima of peak E3, E4, P5 and H1 as function of filling temperature.

peak height is to assume a temperature dependent capture cross section. But also competition of various filling processes depending on the temperature is conceivable, e.g. due to metastable defects which are shifted into different states by the current injection as known e.g. from the C_i-P_s complex (see tab. 3.2).

It should be emphasised that the increase of the peak height towards higher starting temperature is a direct consequence of the filling process and not due to the change of time between the filling and the occurrence of the peak, because no significant charge is emitted from an energy level until the characteristic peak temperature is reached.

7.2.4 Fluence Dependence

Fig. 7.30 gives an overview on how the spectra develop with fluence. It can be seen that the main features of the spectra do not change with increasing fluence. As already shown in fig. 7.18 peak P5 can not be seen after low fluence irradiation. In the following the fluence dependence of the dominant peaks E3 and H1/E6 will be discussed.

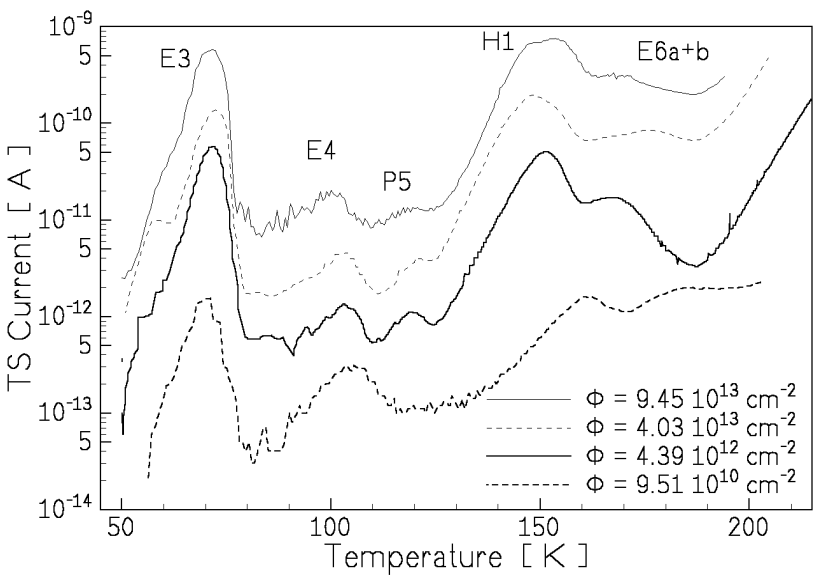

Figure 7.30: TSC-spectra for various fluences. (T_{start}=50 K, I_f=2.5 mA, t_f=21 s, $V_{rev} \approx V_{fd}$).

The fluence dependence of peak E3 is shown in fig. 7.31, where the determined trap concentration is plotted versus fluence. Despite the fluctuation of the data it is evident that two regions can be distinguished. In the low fluence range the trap concentration increases very steeply, while above $\Phi = 1 \cdot 10^{12}$ cm^{-2} the increase is less pronounced but linearly except for the highest fluence. The data are parametrised according to the following equation which has the same form as eqs. 6.13 and 6.14:

$$N_{T,70K}(\Phi) = N_{T,0,70K}(1 - \exp(-c_T\Phi)) + g_T\Phi, \tag{7.6}$$

and the parameters are found to be

$$\begin{aligned} N_{T,0,70K} &= 4.67\ (\pm\ 0.13)\ \cdot 10^{11}\ \mathrm{cm}^{-3}, \\ c_T &= 1.71\ (\pm\ 0.50)\ \cdot 10^{-12}\ \mathrm{cm}^2 \text{ and} \\ g_T &= 0.0287 \pm 0.0007\ \mathrm{cm}^{-1}. \end{aligned}$$

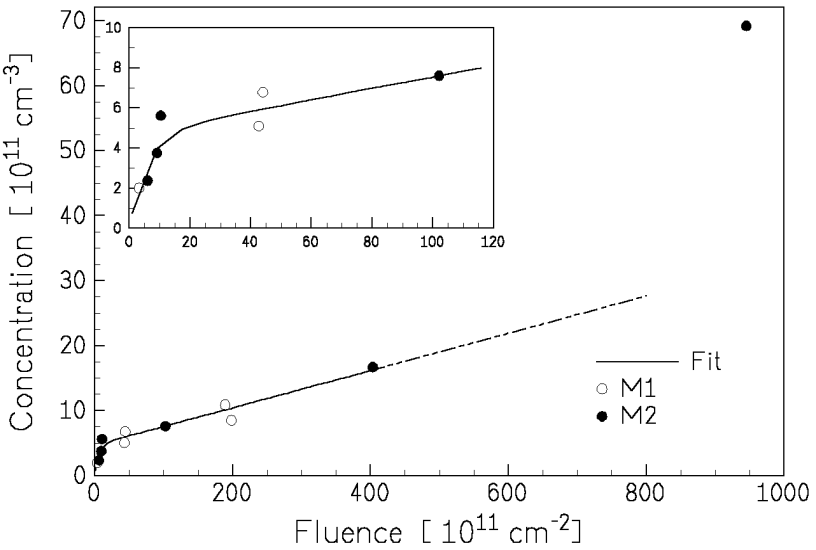

Figure 7.31: Fluence dependence of occupied trap concentration corresponding to peak E3. The inset magnifies the low fluence range. The fit is according to eq. 7.6. Measurement parameters : T_{start} = 50 K, I_f = 2.5 mA, t_f = 20 s.

From $N_{T,0,70K}$ and c_T the generation rate g_{E3} in the low fluence range can be approximated by

$$g_{E3} = N_{T,0,70K} c_T. \tag{7.7}$$

Using the parameters given above it follows $g_{E3} = 0.8\ \mathrm{cm}^{-1}$ consistently with the value obtained from DLTS-measurements with p^+-n -samples (MPI, see p. 133). Trap concentration corresponding to peak E3 found by Biggeri [139] after neutron irradiation using also TSC are significantly smaller especially in the fluence range below $3 \cdot 10^{13}\ \mathrm{cm}^{-2}$. This may be due to the very small filling temperature (8 K) which has been used. A definite physical interpretation which provides an understanding of eq. 7.6 could not be found so far. Certainly it has to be considered that the data shown in fig. 7.31 are determined assuming complete filling and full depletion.

The assumption of complete filling is justified by the results shown in fig. 7.21 and fig. 7.22. The height of peak E3 was found to depend neither on the filling time nor on the filling current.

It has been shown in the preceding section that the depletion voltage at lower temperature can be quite different from the room temperature value. Hence it is conceivable that the data shown in fig. 7.31 reflect the fluence dependence of $N_{SCR}(70K)$ rather than the concentration of A-centres. Assuming the concentration

of A-centres increases in proportion to the fluence in the entire fluence range from the ratio of the measured data $n_{T,false}$ and the calculated values $n_{T,true} = g_{E3}\Phi$ the depletion voltage at $T = 70$ K can be estimated. If $V_{fd}(RT) < V_{fd}(70K)$ the volume of the diode is not fully depleted ($W < d$) and the application of eq. 4.17 leads due to the overestimated volume to an underestimated concentration :

$$n_{T,false} = n_{T,true}\frac{AW}{Ad}. \tag{7.8}$$

Since $n_{T,true} = g_{E3}\Phi$ it is possible to find the depletion depth caused by the applied reverse-bias voltage at 70 K :

$$W_{70K} = \frac{n_{T,false}}{n_{T,true}}d. \tag{7.9}$$

It is furthermore $V_{rev} \propto W^2$ and $V_{fd} \propto d^2$ and thus the depletion voltage at 70 K can be found by :

$$V_{fd}(70K) = V_{rev}\frac{d^2}{W_{70K}^2}. \tag{7.10}$$

The corresponding effective space charge $N_{SCR}(70K)$ is plotted versus fluence in fig. 7.32. In contrast to the values obtained from the M1-samples the behaviour of the M2-data including the high fluence value can be fitted by an exponential term :

$$N_{SCR} = N_{SCR,70K,0}(1 - \exp(-c_{70K}\Phi)). \tag{7.11}$$

with following parameters:

$$\begin{aligned} N_{SCR,70K,0} &= 1.85\ (\pm\ 0.11)\ \cdot 10^{14}\ \mathrm{cm}^{-3} \text{ and} \\ c_{70K} &= 3.8\ (\pm\ 0.10)\ \cdot 10^{-14}\ \mathrm{cm}^{2}. \end{aligned}$$

But two objections have to be made concerning the discussion outlined above :

1.) The value found for $V_{fd}(70K)$ from the experiment discussed in sec. 7.2.3 deviates significantly from the prediction according to eq. 7.11. From fig. 7.27 the depletion voltage of sample M10611 can be estimated to about 64 V, while the application of eqs. 7.8 to 7.10 leads to $V_{fd}(70K) =$ of about 1500 V !

2.) Instead of eq. 7.6 it is now eq. 7.11 which lacks a meaningful physical interpretation.

But anyway, the difference of $V_{fd}(RT)$ and $V_{fd}(70K)$ is caused by charge carriers trapped in the defect-centres. Since all levels emit the charge during the TSC-measurement, the depletion voltage changes continuously during the measurement. In case of low defect concentrations this effect can be neglected, but after high fluence irradiation this effect has strong implications on the evaluation of the defect concentrations.

It is not evident from the fluence dependence if peak E3 is caused by A-centres alone or in combination with C_i-C_s complexes.

As already shown in the introduction (sec. 7.2.1) the peak structure at about 150 K can be recalculated using the results from the DLTS analysis. In order to get the fluence dependence of the corresponding trap-levels the following level parameters were used to fit the spectra by varying only the trap concentrations :

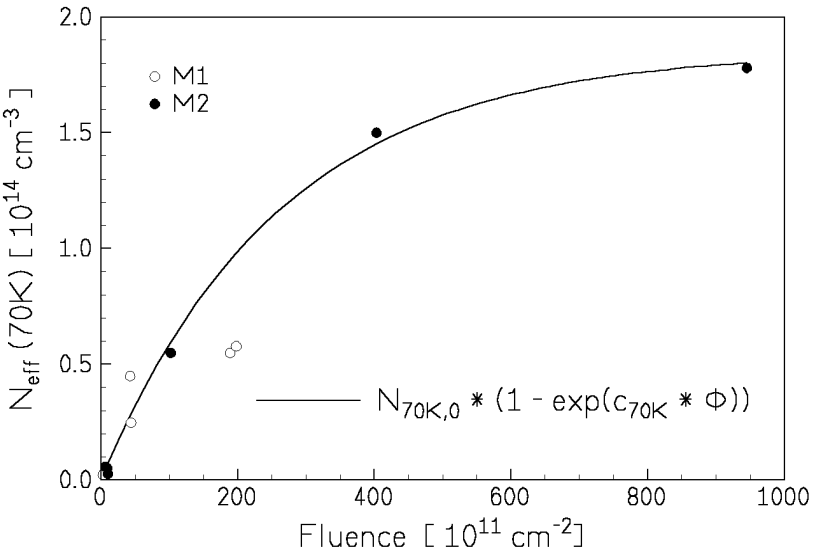

Figure 7.32: Effective space charge at 70 K vs. fluence according to eq. 7.11. Only data of M2-samples were fitted.

Label	ΔE_T	$\sigma_{n,p}$
H1	+0.37 eV	$8.0{\cdot}10^{-15}$ cm^2,
E6a	-0.39 eV	$1.2{\cdot}10^{-15}$ cm^2,
E6b	-0.42 eV	$1.0{\cdot}10^{-15}$ cm^2.

The result is shown in fig. 7.33. Up to $\Phi = 1.9{\cdot}10^{13}$ cm^{-2} the recalculated spectra match the measurements very well. But for fluences above the growth of a further component on the right side of peak H1 occurs, which can not be described by the above given trap level parameters. Nevertheless a 'fit by eye' has been applied without introducing a fourth level.

The trap-concentrations used for the fits plotted versus fluence are also shown in fig. 7.33. Note that the fluence dependence of the trap corresponding to H1 looks very similar to the fluence dependence found for E3. A strong increase is followed by a moderate one and the value obtained for the highest fluence is extremly high again. But due to the occurence of a fourth level and the corresponding uncertainty a fit according to eq. 7.11 has been omitted. The generation rates are calculated as average of individual ratios n_T/Φ. A comparison with the generation rates obtained by DLTS shows that the values determined by TSC are smaller. Similar reasons as given for the behaviour of the E3 trap concentration may be responsible.

Because trap filling was not reproducible in case of the SB-samples a systematic investigation has not been performed. Nevertheless, for comparison and demonstration also two spectra of SB-samples are shown in fig. 7.34. One sample is inverted to p-type, while the other is still n-type. Although a filling voltage of 500V (!) has been applied only a filling current of $I_f = 20$ μA was achieved in case of the inverted sample, while the current through the not inverted one was as high as $I_f = 2$ mA.

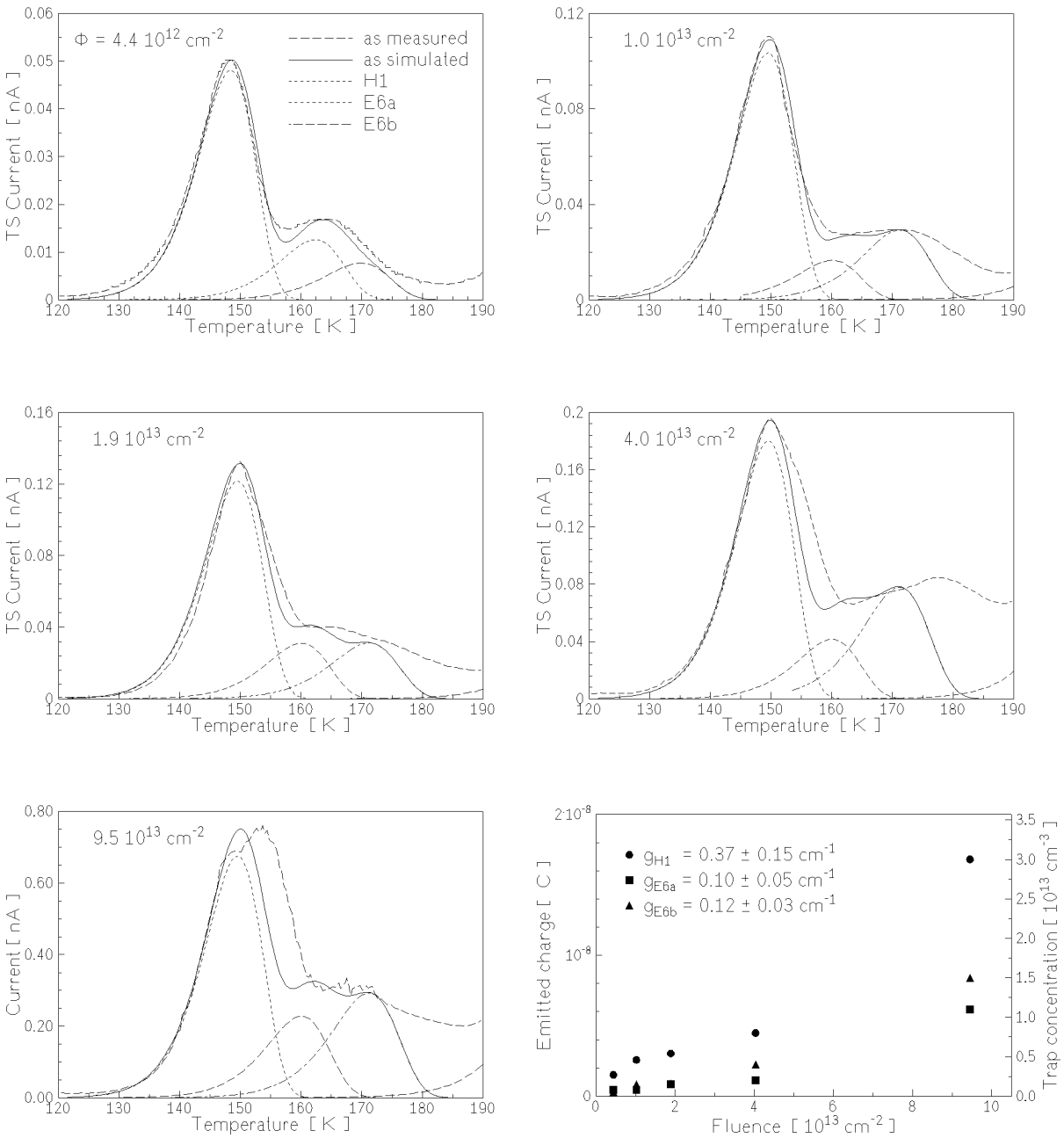

Figure 7.33: Double peak simulated applying results from DLTS for various fluences. The trap concentrations are calculated assuming full depletion.

Hence the height of the peaks must not be compared directly. In both spectra a pronounced peak occurs at 135 K that has not been observed with p^+-n samples. It is also worth to mention that peak E3 in the spectrum of the inverted SB-sample is rather high. Although only a small filling current could be injected the concentration of occupied traps is as high as n_T=2.3·10^{12} cm^{-3}. In contrast the corresponding concentration determined from the M20708-spectrum is only 1.7·10^{12} cm^{-3}, although the sample has been exposed to a fluence which was two times higher.

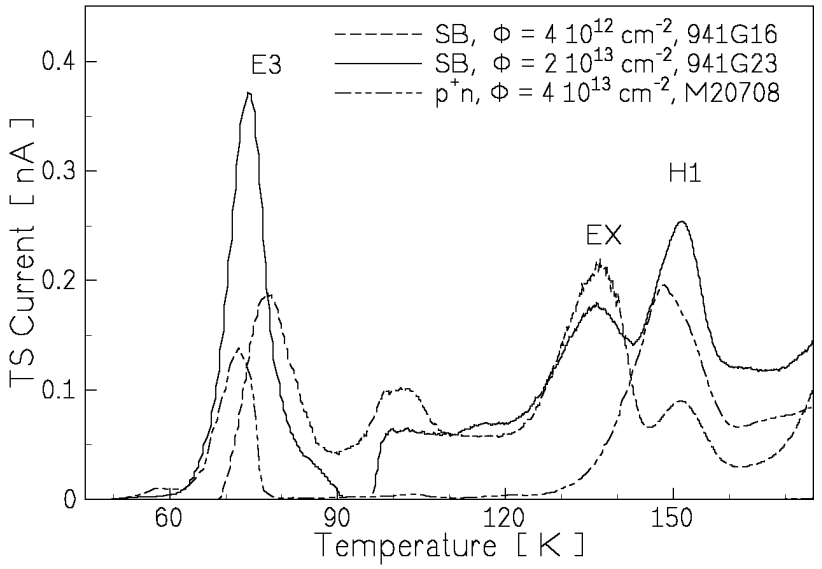

Figure 7.34: TSC-spectra of SB-samples. Sample 941G16 is not inverted, but sample 941G23. The peak which has not been found in the spectra of p^+-n -samples is denoted as EX. For demonstration the spectrum of p^+-n -sample M20708 is also shown. Note that peak E3 in the 941G23-spectrum is rather high in comparison to the peak measured with the p^+-n -sample. The shift of the peak E3 is probably due to an error of the temperature measurement.

7.2.5 Isothermal Tempering

An isothermal heat treatment has been applied to sample MUEA06. The sample was tempered three times at 350 K ($\approx$ 75°C). The tempering times are listed in tab. 7.11. The change of the spectrum due the heat treatments is shown in fig. 7.35. The measurements recorded after current injection at 35 K undergo significant changes only in the temperature range above 140 K, while in the lower temperature range only little changes are visible. In contrast the measurements recorded after current injection at 50 K show a significant increase of peak E3 correlated with the tempering time. This is shown more detailed in fig. 7.36. The increase of the corresponding trap concentration n_T is listed in tab. 7.11. It has to be emphasised that the value of n_T before the tempering procedure is rather small if compared to the data shown in fig. 7.31. Also listed are the effective space charge N_{eff} and the ratio of the change